The distribution of disorientation angles in a rolled AZ31 Mg alloy(•)

J.A. del Valle*,**, M.T. Pérez-Prado** and O.A. Ruano**

Abstract In this work the distribution of disorientation angles corresponding to a rolled AZ31 Mg alloy has been measured and compared with several disorientation distributions calculated for an aggregate of hexagonal crystals using a Monte Carlo simulation method (random sampling). Simulated distributions correspond specifically to: (a) a random aggregate, (b) an aggregate with a perfect basal fiber texture, (c) with a perfect prismatic fiber texture and (d) a polycrystal where neighbour grains is allowed to be disoriented randomly with a condition that the angle between the c-axis be lower than 30°.

Keywords Hexagonal crystals. Grain boundaries. Disorientation angle. Random distribution.

Distribución de ángulos de desorientación en la aleación de Mg laminada AZ31

Resumen En este trabajo, se ha medido la distribución de ángulos de desorientación en una aleación de Mg AZ31 laminada. Los resultados obtenidos se han comparado con varias distribuciones calculadas para un agregado de cristales hexagonales, mediante el método de simulación de Monte Carlo. En particular, se ha calculado la distribución correspondiente a: (a) un policristal con granos orientados al azar, (b) con una textura de fibra basal perfecta, (c) con una fibra prismática perfecta y (d) un policristal donde los granos adyacentes estan desorientados al azar, con la restriccion de que el ángulo entre los ejes c sea menor que 30°.

Palabras clave Cristales hexagonales. Fronteras de grano. Ángulo de desorientación. Distribución al azar.

1. INTRODUCTION

Alloys of hexagonal crystal structure such as Ti, Zr based materials are profusely used for aerospace and nuclear applications. Others such as Mg based alloys have recently attracted much attention due to their potential to replace heavier materials in some automobile parts[1]. It is well known that mechanical properties depend on microstructural parameters such as grain size, texture and grain boundary structure. In particular, the essential role played by grain boundaries has been lately emphasized[2 and 3]. However, there are so far relatively few studies on the grain boundary character of hexagonal polycrystals.

Grain boundary misorientation is commonly described by means of the angle/axis pair descriptor[2]. For a specific misorientation there are several crystalographically related, mathematically equivalent angle/axis pairs (24 for cubic crystals and 12 for hexagonal crystals). By convention the pair with the smallest misorientation angle is selected. This angle is then termed "disorientation angle" (ϕ_m).

The distribution of angles corresponding to a random aggregate of cubic crystals, known as Mackenzie distribution[4-6], has proven to be very useful in assessing the degree of departure from randomness of a given polycrystal[1]. Previous work on the disorientation distributions of random aggregates of crystals with different symmetries can be found in[7-9]. However, to the authors knowledge, only very few studies comparing simulated distributions with experimental results have been yet published[10].

(•) Trabajo recibido el día 5 de noviembre de 2002 y aceptado en su forma final el día 21 de noviembre de 2002.
(*) Consejo Nacional de Investigaciones Científicas y Técnicas (CONICET), Instituto de Física de Materiales Tandil (IFIMAT), Argentina.
(**) Dept. of Physical Metallurgy, Centro Nacional de Investigaciones Metalúrgicas (CENIM). Avda. Gregorio del Amo, 8. 28040 Madrid, Spain. Fax: +34 91 534 7425. E-mail: tpprado@cenim.csic.es

In the present work, the distribution of disorientation angles has been measured for an AZ31 alloy in the as-rolled condition and is compared with several simulated disorientation distributions: those corresponding to an aggregate of randomly oriented hexagonal crystals, to prismatic and basal fibers and to a mixed case. These distributions were calculated by the method of random sampling (Monte Carlo method) developed by Mackenzie and Thomson in its seminal work for cubic crystals[4].

2. EXPERIMENTAL

The AZ31 alloy studied was received as-rolled in the form of a sheet, 1.6 mm in thickness. The main alloying elements in this Mg-based alloy are: Al (3 %) and Zn (1 %).

Macrotexture analysis was performed in a Siemens D5000 diffractometer furnished with a closed eulerian cradle. Sample preparation for macrotexture examination included mechanical polishing with SiC papers up to a grit size of 4000 and final polishing using a solution of colloidal silica.

Electron Backscattered Diffraction (EBSD) measurements were carried out in the as-received and processed samples in a JEOL SEM operating at 20 kV. The Orientation Imaging Microscopy INCA software utilized was provided by Oxford Instruments. EBSD allowed additionally measuring of the disorientation angle distribution. Sample preparation for EBSD is difficult since, due to the low density of Mg, Kikuchi diffraction patterns have very low intensity. Therefore a good surface preparation is crucial. Sample prepeparation consisted on grinding on SiC papers of grit size 400, 600, and 1200, followed by mechanical polishing using 6mm, 3mm and 1mm diamond powders. Final mechanical polishing was achieved with a 0.05 mm alumina solution. Electropolishing was carried out with a solution of 40 % ortophosphoric acid and 60 % ethanol at 2 °C and using a voltage of 2-3 volts. Finally, samples were cleaned with cold ethanol and dried with Ar flow.

3. DESCRIPTION OF THE CALCULATIONS

In the following, the calculation method for the distribution of angles is described. Consider, for example, two hexagonal cells: A (Fig. 1a) is a fixed reference cell and B (Fig. 1b) is rotated with respect to A. Imagine two orthonormal coordinate

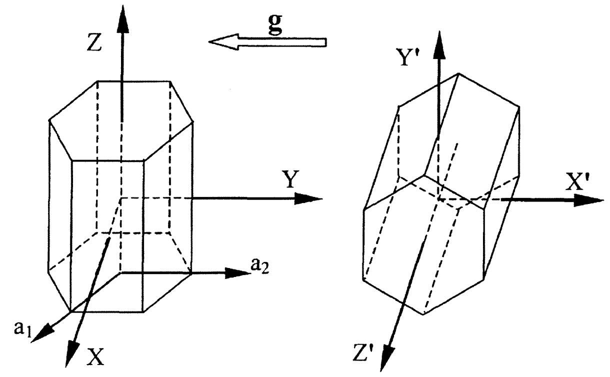

Figure 1. Description of the problem. Schematic showing (a) a reference hexagonal unit cell A with a fixed orthogonal coordinate system {X,Y,Z} and (b) a unit cell B rotated with respect to A.

Figura 1. Descripción del Problema: Esquema que describe (a) una celda hexagonal de referencia con un sistema de coordenadas {X,Y,Z} fijo a ella, y (b) una celda B rotada con respecto a A.

systems fixed to the cells ({X, Y, Z} in cell A and {X', Y', Z'} in cell B) as depicted in figures 1a and b. It is convenient to adapt the choice of the coordinate system to the crystal symmetry. Therefore, the orthonormal axes {X, Y, Z} and {X', Y', Z'} were chosen to coincide with the hcp crystallographic directions [10-10], [-12-10], [0001] in both cells. Having specified the coordinate systems, the rotation which restores B into coincidence with A is given by the rotation matrix **g**. The columns of this matrix are the direction cosines of the angles between corresponding axes of the A and B coordinate systems as explained in[2]. There are 12 different rotations which will restore crystal B into coincidence with A because there are 12 symmetrically equivalent ways of locating the coordinate systems. Therefore there are 12 equivalent rotation matrices $\mathbf{gS}_i$, where $\mathbf{S}_i$ (i = 1...12) are the proper 12 hexagonal symmetry operations given in Appendix By convention the smallest misorientation angle is selected, this angle (termed the disorientation angle ϕ_m) is given by[4 and 5]:

$$1+2\cos\phi_m = \mathrm{Max}[\mathrm{Tr}(\mathbf{gS}_i)] \qquad (4)$$

where $\mathrm{Max}[\mathrm{Tr}(\mathbf{gS}_i)]$ is the maximum of the trace of the $\mathbf{gS}_i$ matrices.

For example, the angle that describes the rotation between cell B and cell A of figure 1 using a rotation matrix $\mathbf{gS}_1$ is 120°. However, the smallest angle that describes the rotation between cell B and cell A is obtained using a rotation matrix $\mathbf{gS_2}$, leading to 93.84°, therefore $\phi_m = 93.84°$.

In order to reduce the noise and obtain a distribution given by a smooth curve, a large number of rotation matrices **g** must be first generated. In this work a total of 10^6 rotation matrices were constructed as follows. Any rotation matrix **g** can be represented by a 3 × 3 orthogonal matrix. The elements in successive columns of these matrices can be regarded as the components of three orthogonal unit vectors. A random unit vector can be written in the form[4]:

$$\left[\left(1-\xi^2\right)^{1/2}\cos\varphi, (1-\xi^2)^{1/2}\sin\varphi, \xi\right] \qquad (5)$$

where ξ is chosen at random in the range (-1,1) and the longitude φ is chosen simultaneously at random in the range $(-\pi,\pi)$. In this way the vectors obtained are uniformly distributed on a sphere of radius 1. The matrix construction process start by the generation of a random vector $\boldsymbol{v_1}$, and its components are written as the first column of **g**. Next a second random vector $\boldsymbol{w}$, independent of $\boldsymbol{v_1}$, is generated. These two vectors define a random plane. Within this plane, a vector $\boldsymbol{v_2}$ normal to $\boldsymbol{v_1}$ is given by:

$$v_2 = \left[(w_x\text{-}Pv_{1x}), (w_y\text{-}Pv_{1y}), (w_z\text{-}Pv_{1z})\right] / [1\text{-}P^2]^{1/2} \quad (6)$$

where $P = \boldsymbol{v_1}.\boldsymbol{w}$. The components of the vector $\boldsymbol{v_2}$ are written in the second column of the matrix **g**. Finally, the remaining column of **g** is obtained by computing $\boldsymbol{v_3} = \boldsymbol{v_1} \times \boldsymbol{v_2}$.

For each rotation matrix **g**, the products $\mathbf{gS_i}$ were calculated and the disorientation angle f_m was obtained by calculating $\mathrm{Max}[\mathrm{Tr}(gS_i)]$. With these data a normalized frequency histogram with class interval of 0.5° can be constructed. A solid line probability distribution, therefore, can be drawn through these points.

4. RESULTS AND DISCUSSION

Several disorientation distributions were calculated by the method described above. These distributions can then be used to analyze measured distributions corresponding to hexagonal polycrystals, as will be done below for the as-received AZ31 alloy under study. The normalized simulated distributions are depicted in figure 2. Figure 2a illustrates the distribution of disorientation angles corresponding to an hexagonal polycrystal with a perfect basal or prismatic fiber texture. In the case of the basal fiber texture the crystals are allowed to rotate around the c-axis at random in the range $(-\pi,\pi)$. It can be seen that the disorientation angle probability is uniform between 0° and 30°. The rotation axis coincides with the c-axis. The same probability distribution was found for a prismatic (10-10) and a prismatic (11-20) fiber texture. The disorientation angle probability is uniform between 0° and 90°. Figure 2b shows the distribution corresponding to a random aggregate of hexagonal crystals which has a maximum at 90° and the maximum angle allowed, or cut-off value, is 93.84°. This cut-off value corresponds to the rotation between cell B and cell A of the example of figure1. This result is in agreement with previous work on the disorientation distributions of random aggregates[7-9].

In real materials perfect fibers are only very rarely observed. Instead, less well defined, more spreaded fibers are more common. In an attempt to describe this class of fibers the disorientation distribution was calculated by means of the generation of random rotations for the cell B, and choosing the subgroup of rotations that fulfill the additional condition that the angle between the c-axis of cells B and A, called θ, remains lower than 30°. In such way, the distribution calculated corresponds to a basal fiber where neighbour grains have the c-axis at angles lower than 30°. This distribution, illustrated in the figure 2b, has a maximum at 30° and the cut-off value is 42.3°.

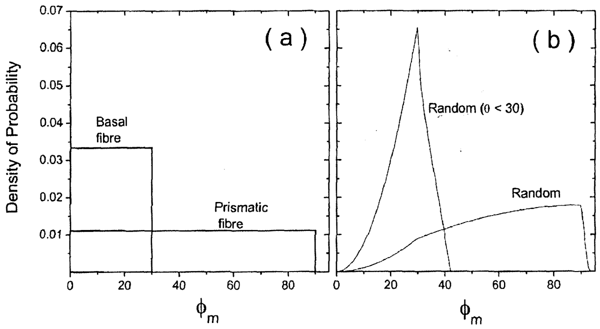

Figure 2. (a) Probability distribution vs. disorientation angle corresponding to an aggregate of hexagonal crystals with basal or prismatic fiber texture (b) Probability distribution of random aggregate, and of a restrained (θ < 30°) random aggregate of hexagonal crystals.

Figura 2. (a) Distribuciones de Probabilidad vs. ángulo de desorientación correspondientes a un agregado de cristales hexagonales con textura de fibra basal o prismática. (b) Distribución de Probabilidad para un agregado policristalino aleatorio, y para un agregado aleatorio restringido (q < 30o) de cristales hexagonales.

Figures 3a and 3b show the measured (0002) pole figure (macrotexture) and the measured probability distribution of disorientation angles corresponding to the as-received AZ31 alloy under study. It can be seen in figure 3a that the texture of this material in the as-received condition is formed by a basal fiber with some spread around the normal to the rolling plane (ND). The measured disorientation distribution has a peak at 30°. This suggests a resemblance with the distribution simulated for a basal fiber with a spread of 30°. Some divergences exist, however, between the simulated and measured distributions: the latter shows a higher probability for disorientation angles higher than 40° and a lower peak height at 30°. This divergence can be attributed to the presence of a small fraction of randomly oriented grains. As shown in figure 3.a there is some population of grains whose c-axis is rotated more than 30° from the normal to the rolling plane (ND).

5. SUMMARY AND CONCLUSIONS

A Monte-Carlo method based on previous work by MacKenzie[4-5] has been used to simulate disorientation distributions in an aggregate of hexagonal crystals. Using this methodology several disorientation distributions corresponding to different textures have been simulated: (a) perfect basal fiber texture; (b) perfect prismatic fiber texture; (c) random texture; and (d) a spread fiber texture in which the c-axis is allowed to rotate 30° with respect to the normal to the rolling plane (ND). The results have been compared with those measured in a AZ31 alloy in the as-received as-rolled condition. A fairly good agreement was found between the measured data and the simulated distribution corresponding to a spread fiber. The divergences between both distributions can be attributed to a small volume fraction of randomly oriented crystals that was not considered in the calculations. The methodology described in the present paper can be utilized as a tool for analysis of mesotextures of polycrystals.

Appendix

Matrix representation of the 12 proper symmetry operations in the hexagonal lattice.

Acknowledgements

Financial support from the Consejo Nacional de Investigaciones Científicas y Técnicas (CONICET), Argentina, from the Ramón y Cajal program, MCYT, Spain, and from a CICYT grant MAT 2000-1313, Spain, is acknowledged.

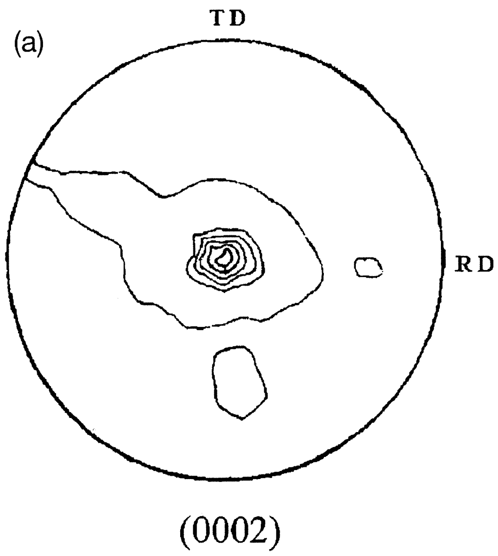

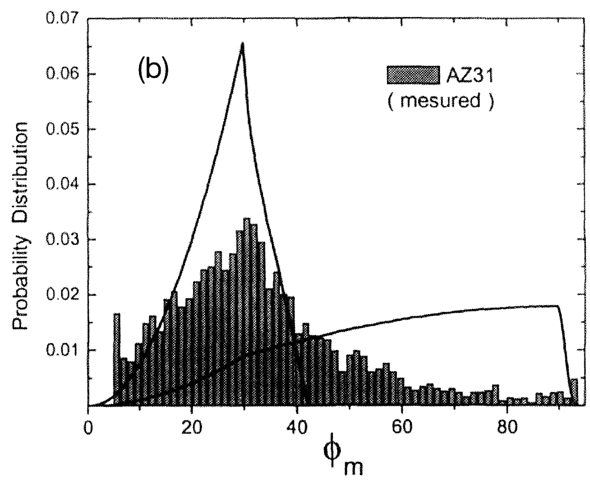

Figure 3. (a) (0002) pole figure corresponding to the as-received AZ31 alloy. A basal fiber can be clearly appreciated. (b) Measured probability distribution of disorientation angles compared with the theoretical distributions of figure 2.b.

Figura 3. (a) Figura de polos (0002) correspondiente a la aleación AZ31 recibida. La fibra basal puede apreciarse claramente (b) Se compara la Distribución de Probabilidad de ángulos de desorientación medida con las distribuciones teóricas de la Figura 2.b.

$$S_1 = \begin{pmatrix} 1 & 0 & 0 \\ 0 & 1 & 0 \\ 0 & 0 & 1 \end{pmatrix} \quad S_2 = \begin{pmatrix} 0.5 & 0.866 & 0 \\ -0.866 & 0.5 & 0 \\ 0 & 0 & 1 \end{pmatrix} \quad S_3 = \begin{pmatrix} -0.5 & 0.866 & 0 \\ -0.866 & -0.5 & 0 \\ 0 & 0 & 1 \end{pmatrix}$$

$$S_4 = \begin{pmatrix} -1 & 0 & 0 \\ 0 & -1 & 0 \\ 0 & 0 & 1 \end{pmatrix} \quad S_5 = \begin{pmatrix} -0.5 & -0.866 & 0 \\ 0.866 & -0.5 & 0 \\ 0 & 0 & 1 \end{pmatrix} \quad S_6 = \begin{pmatrix} 0.5 & -0.866 & 0 \\ 0.866 & 0.5 & 0 \\ 0 & 0 & 1 \end{pmatrix}$$

$$S_7 = \begin{pmatrix} 1 & 0 & 0 \\ 0 & -1 & 0 \\ 0 & 0 & -1 \end{pmatrix} \quad S_8 = \begin{pmatrix} 0.5 & 0.866 & 0 \\ 0.866 & -0.5 & 0 \\ 0 & 0 & -1 \end{pmatrix} \quad S_9 = \begin{pmatrix} -0.5 & 0.866 & 0 \\ 0.866 & 0.5 & 0 \\ 0 & 0 & -1 \end{pmatrix}$$

$$S_{10} = \begin{pmatrix} -1 & 0 & 0 \\ 0 & 1 & 0 \\ 0 & 0 & -1 \end{pmatrix} \quad S_{11} = \begin{pmatrix} -0.5 & -0.87 & 0 \\ -0.87 & 0.5 & 0 \\ 0 & 0 & -1 \end{pmatrix} \quad S_{12} = \begin{pmatrix} 0.5 & -0.866 & 0 \\ -0.866 & -0.5 & 0 \\ 0 & 0 & -1 \end{pmatrix}$$

REFERENCES

[1] B.L. MORDIKE and T. EBERT, *Mater. Sci. Eng.* 302 (2001) 37-45.

[2] V. RANDLE and O. ENGLER, *Introduction to Texture Analysis: Macrotexture, Microtexture and Orientation Mapping*, Gordon and Breach, Amsterdam, 2000.

[3] T. WATANABE, *Proc.* ICOTOM 13, *Mater.Sci. Forum* 408-412 (2002) 39-48.

[4] J.K. MACKENZIE and M.J. THOMSON, *Biometrika* 3 (1957) 205-210.

[5] J.K. MACKENZIE, *Biometrika* 45 (1958) 229-240.

[6] J.K. MACKENZIE, *Acta. Metall.* 12 (1964) 223-225.

[7] H. GRIMMER, *Scrip. Metall.* 13 (1979) 161-164.

[8] A. MORAWIEC, *Acta Cryst.* 53 (1997) 273-285.

[9] A. MORAWIEC, *J. Appl. Cryst.* 29 (1996) 164-169.

[10] D.I. KIM, J.H. LEE, K.H. OH and H.C. LEE, *Mater. Sci. Forum* 408-412 (2002) 1699-1704.